Performance comparison of some weak signal detection techniques

Sarah Sabah Mohammed, Maher K. Mahmood Al-Azawi
Department of Electrical Engineering, Faculty of Engineering, Al-Mustansiryah University, Baghdad, Iraq

Article Info

ABSTRACT

Performance comparison of some weak signal detection techniques is introduced. This comparison is very necessary since different applications require different operating conditions such as signal-to-noise ratio (SNR), bandwidth, coherency, processing time and complexity. Three methods for detecting weak signals are considered. These are based on chaos theory, wavelet transform, and stocastic resonance. A detection algorithm based on a rectangular region in phase space plane is suggested in chaos method. The stocastic resonance method is considered in this research, as it is used for signal detection in underwater at a certain frequency. Simulation results obtained from MATLAB programs verify the studied methods giving an estimation of probability of detection and probability of false alarm versus SNR.

Corresponding Author:

Sarah Sabah Mohammed
Department of Electrical Engineering, Faculty of Engineering, Al-Mustansiriyah University
Baghdad, Iraq
Email: eema1036@uomustansiriyah.edu.iq

1. INTRODUCTION

Recently, there has been an increase in studies on detecting weak signals in a strong noise environment. A weak signal is a signal that has a negative signal-to-noise ratio, which means that the signal level is smaller than the noise level. Applications of weak signal detections include very long-distance communication, snooping purposes, pipeline leakage, seismic testing, acoustic telemetry systems, war fields, radar, sonar, fault diagnosis of mechanical system, industrial measurement and underground/underwater communication. The comparison between different detection techniques is based on the required SNR, bandwidth, coherency, processing time, and complexity. This comparsion is very necessary since the requirements in each application are different.

One of the methods used to detect weak signals is chaos theory using Duffing equation. This equation is used to detect very weak signals based on the very high sensetivety of chaotic system [1]–[7]. However, detecting a weak signal without knowing the signal's information is a major problem that can be solved using wavelet transform. Wavelet can identify local signal properties and perform multiresolution analysis using scaling and translation in both time and frequency domains. It breaks down the signal plus noise into a succession of sub-bands with various spatial resolutions, frequency characteristics, and direction characteristics [8]–[16].

Stochastic resonance is a fascinating physical nonlinear phenomena that occurs when noisy signals have an increased signal-to-noise ratio (SNR) output under particular conditions. Since it is suggested by Benzi *et al*. [17], it has large interest in a wide range of research fields, including electrical, optical, physical, biological sciences, and as an advanced signal processing method [17], [18]. The effective SNR is increased by increasing the energy of weak signal and reducing noise energy at a certain resonance frequency [19]-[29].

In this paper, chaotic, wavelet, and stochastic resonance methods are implemented and compared. A suggestion to improve the performance of chaotic method is also introduced. Comparsions are made based on probability of detection and probability of false alarm for different SNR ranges. The remainder of the paper is organized as: Section 2 discusses some weak signal detection techniques; section 3 discusses the simulation results of the aforementioned techniques; section 4 gives some conclusions.

2.   SOME WEAK SIGNAL DETECTION TECHNIQUES
2.1. Chaotic detection system
2.1.1 Basic model (Duffing Holmes oscillator)
The main principle of detecting weak signals is based on Duffing-Holmes oscillator 2nd order differential as (1).

$$x'' + \gamma x' - x + x^3 = d\cos(t) \tag{1}$$

Where, γ is a damping ratio and $d\cos(t)$ is the periodic reference signal of the system, $-x + x^3$ is the nonlinear restoring force. After fixing γ value, d can range from tiny to large values, and the system state can range from modest periodic motion to chaotic motion, and finally huge periodic motion. The phase transition from chaos to big periodic motion is employed in this research to determine whether there is any signal hidden in the noise [3], [4]. The value of d is fixed to d_{cr} (d_{cr} is a term that refers to a critical value), so the system is put into the critical state. As a result, the chaos system is on the edge of transitioning to periodic motion. The detected signal can be thought of as a deviation from the main sinusoidal driving force, $d\cos(t)$ (the reference signal). Despite the fact that noise can be very large, it can only influence the local trajectory on the phase plane diagram, not create phase transitions. When a signal s(t) has the same frequency as the reference signal, it is buried in noise [5]. As a result, if d exceeds d_{cr}, a phase transition will occur, and the large periodic motion will draw it out of the background noise.

The transformation from chaos to regularity is highly difficult if the difference in frequency between the weak signal and the reference signal is too large, and the degree of difficulty is nearly equal to the level of noise. This represents a single oscillator's selectivity, i.e. one oscillator can only detect its close frequencies. To detect signals with unknown frequencies, an array of oscillators must be utilized. The chaotic system has a sensitive dependence on initial conditions, which means that even if the initial conditions are somewhat changed, the chaotic signals produced are extremely different. Time series and phase diagrams from the numerical solution of the Duffing-Holmes equation is shown in Figure 1. Figure 1(a) shows the chaotic motion while Figure 1(b) shows the great periodic motion. Hence, the detection model designed as (2).
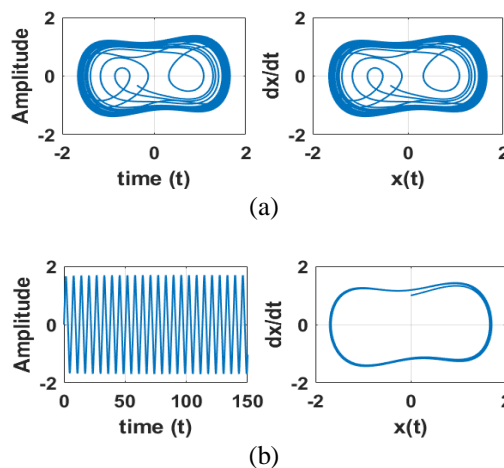

Figure 1. Time series and phase diagrams of chaotic system of (a) time series and phase diagram of chaotic motion and (b) time series and phase diagram of great periodic motion

$$x'' + \gamma x' - x + x^3 = d\cos(t) + Input \tag{2}$$

$Input = s(t) + n(t), s(t) = A\cos(wt)$ is the signal to be detected and $n(t)$ is additive white Gaussian noise (AWGN) with variance σ^2 and the SNR$= A^2/2\sigma^2$.

2.1.2 Detection model

Often Lyapunov exponent (LE) method is used to specify the parameters of the system and also calculate the optimum threshold value to detect the weak signal. However, this method is complicated and takes a very long time in simulation. To solve this problem, another method called the rectangular-method is suggested. This depends on recognizing the detection from the phase-space plane. Figure 2 shows this rectangular window where Figure 2(a) shows the case of no detected signal while Figure 2(b) shows the case for signal being detected. If absolute of x(t) is less than k_1 and absolute of x'(t) is less than k_2, the points will be inside a rectangle bounded by k_1 and k_2, otherwise it will be outside this rectangle. Depending on the above conclusion, calculation is done to find the percentage of points inside the rectangular area to the total points introduced from the numerical solution. Then, the resulting values are compared with a threshold to determine if the signal is present or not. The threshold value is related to the probability of detection P_d and the required probability of false alarm P_{fa}.
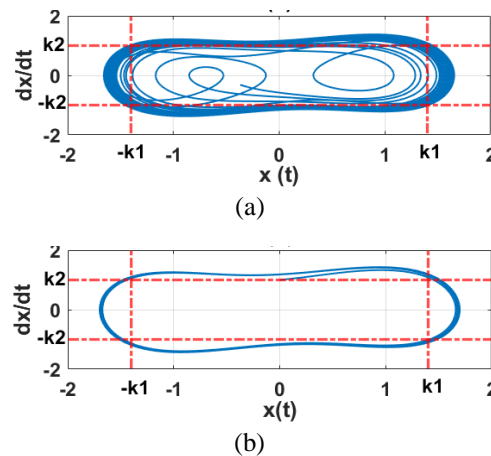

(a)

(b)

Figure 2. Rectangular window in phase plane for chaotic system shape of (a) rectangular window for no detected signal and (b) rectangular window for signal is detected

2.2. Wavelet method

The wavelet transformation is perhaps the best for multi-resolution analysis, as developed by Mallat [8]. The integral transformation in the wavelet transform, on the other hand, is obtained by expanding and shifting basic wavelet functions. The time-frequency signal may be processed since these functions are in time and frequency domains. The criterion and the set of scaled and shifted functions $g_{a,b}(t)$ are satisfied by the wavelet transform, expressed as (3).

$$g_{a,b}(t) = \frac{1}{\sqrt{a}} \, g\left(\frac{t-b}{a}\right)$$ (3)

The scale parameter for scale transformation is 'a', and the shift parameter for shift transformation is 'b', which becomes the wavelet's time domain central location. $1/\sqrt{a}$ is the normalized constant, which ensures that the energy is consistent across all scale parameters. Using the transform coefficient W(a,b), the wavelet transform of function f(t) is given by (4).

$$W(a,b) = \int_{-\infty}^{\infty} f(t) \, \bar{g}_{a,b}(t) \, dt = \frac{1}{\sqrt{a}} \int_{-\infty}^{\infty} f(t) \, \bar{g}\left(\frac{t-b}{a}\right) dt$$ (4)

The complex conjugate is represented by the overbar ($\bar{g}$). The wavelet transform involves time domain signal correlation with the wavelet and frequency domain filtering, and it provides high time resolution for high frequencies and high frequency resolution for low frequencies. The signal is filtered using wavelet transform in both time and frequency domains. Consider the relationship between the signal's time spread and the wavelet's time spread and select the right scale parameter to achieve the best response of the signal's transform coefficients.

The wavelet packet transform is an extension of the discrete wavelet. It's employed in a variety of applications, including noise reduction. The outcome is a low pass (scaling function) and a high pass

(wavelet function) are calculated in one stage of the wavelet transform. The low pass result of the first level is a smoother version (has less noise level) of the original signal $f(t) = s(t) + n(t)$. Recursively, the low pass result becomes the input to the next wavelet layers, which calculate another low and high pass results as shown in Figure 3. The signal detection $s(t)$ in noise $n(t)$ is then calculated from the energy of the low-pass output of the last level and compared with a threshold value to decide the existence of the signal. Again, this threshold value is related to P_d and the required P_{fa}.
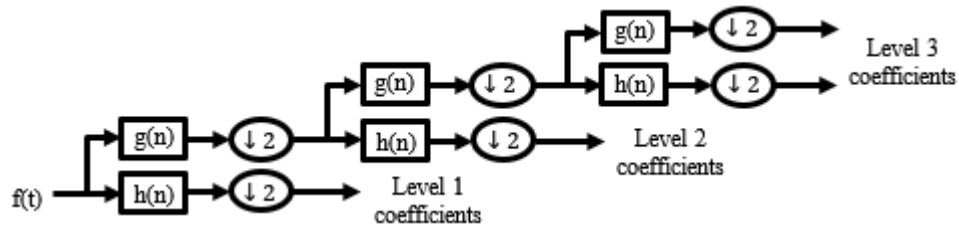
Figure 3. Multi-level discrete wavelet implementation using filter bank

2.3. Stochastic resonance (SR)
2.3.1 Basic model of bistable SR

A stochastic resonance is a nonlinear event in a modulated bistable system or multistable system generated by periodic signals with additional noise. It is illustrated by the second-order nonlinear differential equation [23], expressed as (5).

$$x'' + \gamma \, x' = -V(t)' + s(t) + n(t) \tag{5}$$

Where γ is a damping factor. $s(t) = A\cos(2\pi f_0 t)$ is the weak signal to be detected, where A and f_0 are amplitude and driving frequency, respectively, $n(t) = \sqrt{2D} \, \xi(t)$ with $\langle n(t), n(t + \tau) \rangle = 2D\delta(t)$ stands for the noise, where D is the noise intensity, τ is time delay. V(x) is a potential function given by (6).

$$V(t) = -\frac{a}{2} x^2 + \frac{b}{4} x^4 \, , a, b > 0 \tag{6}$$

In which 'a' and 'b' represent the bistable potential's barrier parameters. As shown in Figure 4, there are two stationary places that are both stable at $\pm x_m = \pm\sqrt{a/b}$ and an unstable one at $x_0 = 0$. The barrier height can be measured as $\Delta v = a^2/(4b)$. The characteristic frequencies to the system are $w_b = [V''(\pm x_m)]^{\frac{1}{2}} = \sqrt{(2a)}$ and $w_0 = [V''(\pm x_0)]^{\frac{1}{2}} = \sqrt{(a)}$. Substitute (6) into (5), then (7).

$$x'' = ax - bx^3 - \gamma \, x' + A\cos(2\pi f_0 t) + \sqrt{2D}\xi(t) \tag{7}$$

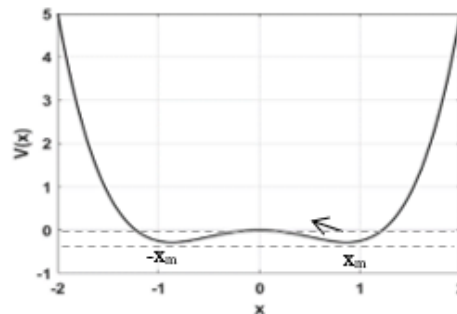Figure 4. Bistable SR system potential V (x)

The system model at (7) can be illustrated in Figure 5, where it can be seen that the measured of SR output x(t) is equal to a secondary integration operation and also equals to a secondary filtering operation.
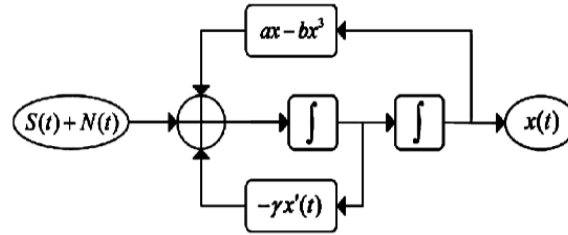
Figure 5. The system model of the underdamped second-order SR

2.3.2 The matching framework based on Kramers rate

The Kramers rate r_K is initially considered as the most important characteristic linked to noise intensity D and driving frequency f_0. When a signal is periodic with suitable noise and a particle's mean passage time is equal to the half-period of the periodical force given to the particle, the stochastic resonance phenomena occurs. The noise and signal are statistically synchronized, resulting in a mild periodic force. The transition particle probabilities agree with Kramers rate r_k, which may be computed as follows [18], expressed as (8).

$$r_k = \frac{w_b w_0}{2\pi\gamma} \exp\left(-\frac{\Delta v}{D}\right) = \frac{a}{\sqrt{2}\pi\gamma} \exp\left(-\frac{\Delta v}{D}\right) = 2f_0 \tag{8}$$

Moreover, define a discrimination function, to the fitness of parameter analyzing $F(a, b, D, \gamma, f_0)$ as [23], expressed as (9).

$$F(a, b, D, \gamma, f_0) = \frac{a}{\sqrt{2}\pi\gamma f_0} \exp\left(-\frac{a^2}{4bD}\right) \tag{9}$$

Clearly, when $F = 1$ is examined in conjunction with both signal frequency and noise intensity, the SR phenomenon occurs, and we get the best relationship between noise intensity and system characteristics. The parameter a=1 can be considered as a modest parameter constraint because the noise intensity is only varied in a narrow range. Then we can have the relationship between 'a', 'b', and γ as shown in (10), (11), and (12).

$$D_{opt} = \frac{a^2}{4b} = \Delta v \tag{10}$$

$$b = \frac{a^2}{4D} \tag{11}$$

$$\gamma = \frac{a^2}{2\sqrt{2}\,\pi\,f_0\,e} \tag{12}$$

Solving (7) for x(t) using Runge Kutta method (RK4), the energy of x(t) is calculated and compared with a threshold to determine if the signal is present or not. Again, this threshold value is related to P_d and the required P_{fa}.

3.   SIMULATION RESULTS
3.1. Detection by Duffing-Holmes's oscillator

Intuitively, the damping factor γ and driving force d play a critical role to obtain the periodic movement necessary for the signal detection process and to achieve the desired optimum output. Therefore, the optimal factors are γ=0.5 and d_{cr}=0.824322 corresponding to the optimal output with noise intensities with initial conditions $x(0) = 0, x'(0) = 1$. To check the chaotic behavior of the system, AWGN noise $n(t) = \sigma\, randn$ (MATLAB m-file function for Gaussian noise) only is added to the equation where σ^2 is the noise variance, and (1) will be (13).

$$x'' + \gamma\, x' - x + x^3 = d\, cos(t) + \sigma\, randn \tag{13}$$

And the system shows a chaotic behavior. However, if the signal to be detected $s(t) = Acos(t)$, is added as in (2), the system will show periodic response due to $s(t)$.

The procedure of obtaining probability of detection (P_d) versus SNR is achieved by repeating this simulation for 1000 times or more. The decision of detection is based on the rectangular window shown in Figure 2. Figure 6 and Figure 7 show system response due to noisy input for SNR=-20 dB and -55 dB respectively. Figure 6(a) shows the pure signal, Figure 6(b) shows the noisy signal for SNR=-20 dB, Figure 6(c) shows the phase representation and Figure 6(d) shows the phase representation for output Duffing oscillator. Also Figure 7(a) shows the pure signal, Figure 7(b) shows the noisy signal for SNR=-55 dB, Figure 7 (c) shows the phase representation and Figure 7(d) shows the phase representation for output Duffing oscillator.

(a)   (b)

(c)   (d)
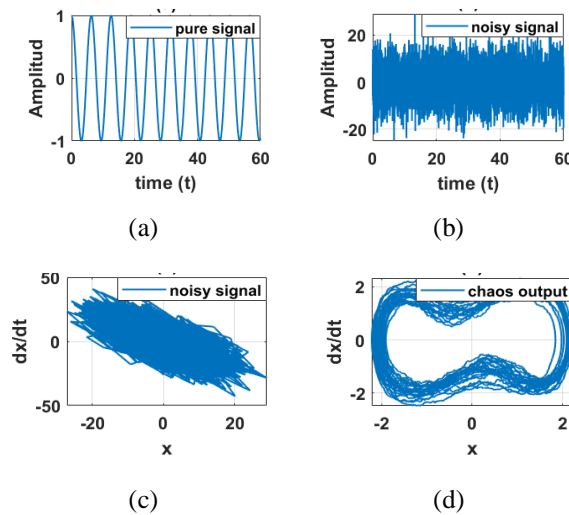
Figure 6. Detection weak signal using chaotic system at SNR=-20 dB of: (a) pure signal wave, (b) noisy signal wave, (c) phase representation for noisy signal, and (d) phase representation for the output of Duffing oscillator
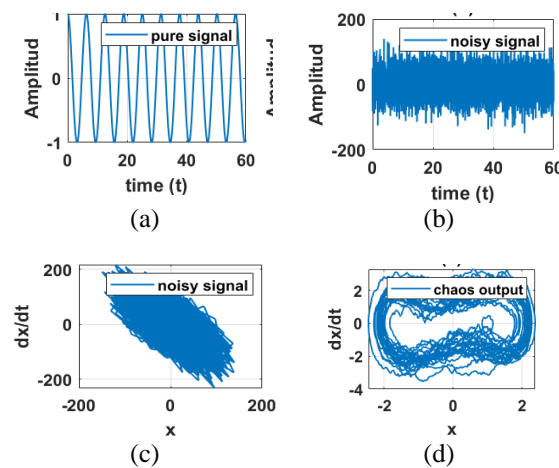

(a)   (b)

(c)   (d)

Figure 7. Detection weak signal using chaotic system at SNR =-55 dB of: (a) pure signal wave, (b) noisy signal wave, (c) phase representation for noisy signal, and (d) phase representation for the output of Duffing oscillator

The performance of probability of detection versus SNR under different P_{fa} is given in Figure 8. The input SNR varies from -80 dB to 0 dB. For P_{fa}=1%, $P_d \approx$100% down to -75 dB while P_d=97% at SNR=-80 dB. For P_{fa}=0.5%, P_d=91% at SNR=-80 dB. To further evaluating the detection performance, the receiver operating characteristic (ROC) curves at SNR=-75 dB and -80 dB are shown in Figure 9. It is noted from previous figures that chaotic method can detect very very weak signals. Hence, the SNR required may be

reduced down to -80 dB due to high sensitivity of chaotic system. The only weak point here is it's dependency on the operating frequency (coherent detection).
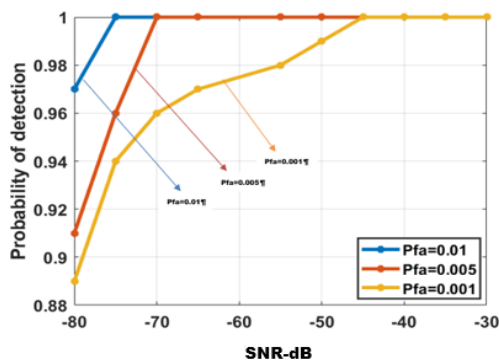

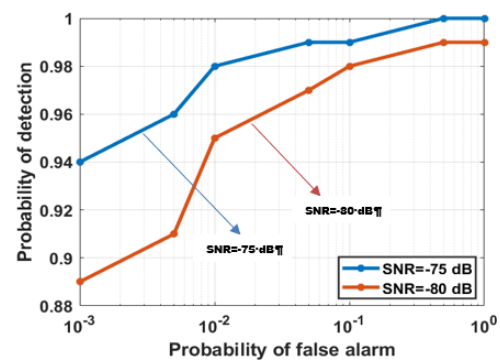Figure 8. Probability of detection versus SNR using Duffing oscillator

Figure 9. ROC curve using Duffing oscillator under SNR=-75 dB and -80 dB

3.2. Detection by wavelet method

By using Debauches wavelet with L-levels of decompositions, the effectiveness of decomposition and reconstruction depends on the number of levels. Figures 10 shows system response to a noisy input signal for SNR=-3 dB. In Figure 10(a) a pure signal is shown. In Figure10(b) a noisy signal is shown after filtering. Figure 10(c) shows the case when L=2. Figure 10(d) shows the case when L=3. Figure 10(e) shows the case when L=4. Figure 10(f) shows the case when L=5.
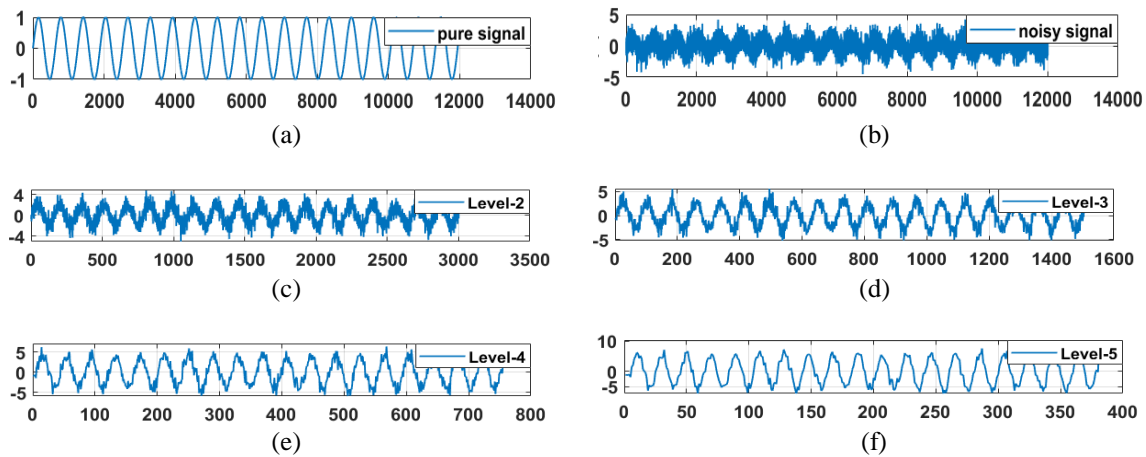

Figure 10. Detection weak signal using discrete wavelet transform (DWT) at SNR =-3 dB for:
(a) pure signa wave, (b) noisy signal; signal wave after filtering, (c) the case when L=2, (d) the case when L=3, (e) the case when L=4, and (f) the case when L=5

Figures 11 shows system response to a noisy input signal for SNR=-13 dB. In Figure 11(a), a pure signal is shown. In Figure 11(b) a noisy signal is shown after filtering. Figure 11(c) shows the case when L=2. Figure 11(d) shows the case when L=3. Figure 11(e) shows the case when L=4. Figure 11(f) shows the case when L=5. These figures display pure signal with number of samples N=12000 and noisy signal as shown in subplot Figure 11(a) and (b). Subplots Figure 11(c)-(f) show the signals after applying wavelet decomposition process to coefficient details and approximate details, for different levels L=2,3,4,5 respectively. It is clear that the noise level decreases with the increase in the wavelet levels and in each stage the time is divided by two.
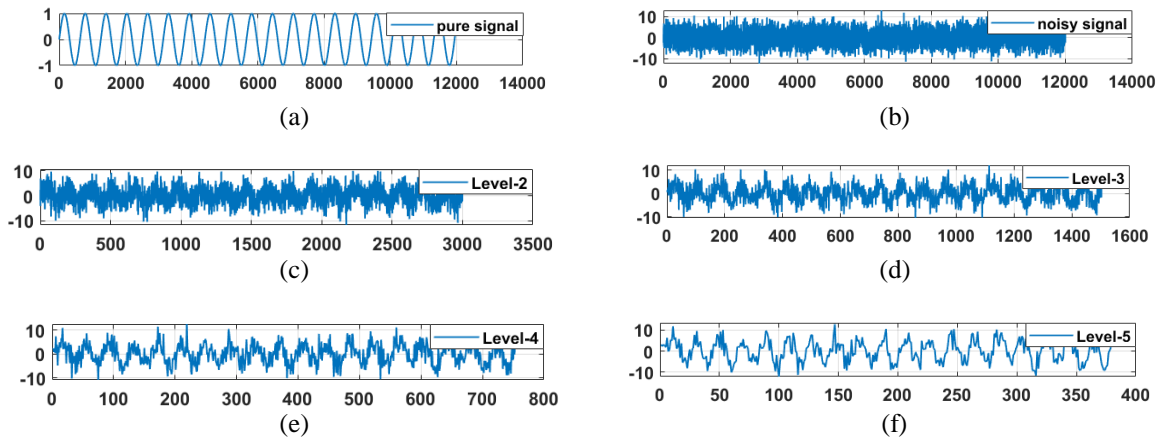
Figure 11. Detection weak signal usind DWT at SNR=-13 dB for: (a) pure signal wave, (b) noisy signal, signal wave after filtering, (c) the case when L=2, (d) the case when L=3, (e) the case when L=4, and (f) the case when L=5

The performance of P_d versus SNR for different levels under different P_{fa} is given in Figure 12. The input SNR varies from -20 dB to 0 dB. As an example, at L=4, the variation of SNR down to -16 dB gives $P_d \approx 100\%$ and at SNR=-18 dB gives P_d=93% at P_{fa}=1%. Less P_d is obtained with the value of 65% at the same SNR and with P_{fa}=0.1%. To further evaluating the detection performance, the receiver operating characteristic curves under low SNR of SNR=-15 dB and -18 dB are shown in Figure 13 for L=3,4,5 respectively. It is noted from previous figures that the wavelet technique can detect signals at SNR down to -20 dB. However, it can detect weak signal irrespective of the operating frequency (noncoherent detection). This is considered as an advantage over previous chaotic method.
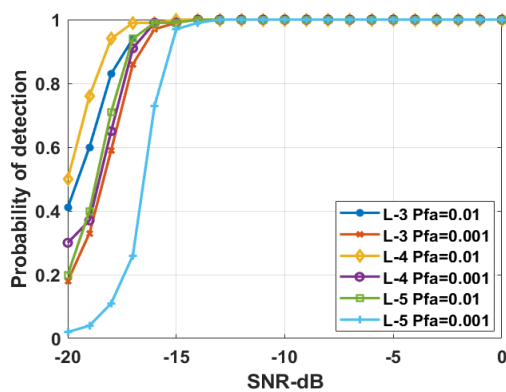

Figure 12. Probability of detection versus SNR using DWT with three levels L=3, L=4, and L=5 according to P_{fa}
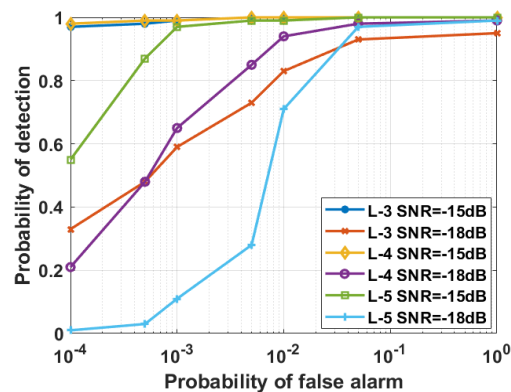
Figure 13. ROC curves of detection using DWT under SNR=-15 and -18 dB, with levels L=3, L=4, and L=5

3.3. Detection by stochastic resonance method

The denoising performance of the   tochastic resonance approach is presented in this subsection. First, (7) is used to find x(t) using a numerical technique, which is based on fourth order Runge-Kutta method (RK4). Figure 14 shows the timing waveforms for SR method. In Figure 14(a), the tested signal is a sinusoid with amplitude A=1 volt and normalized frequency fo=1 Hz, and the data length (number of samples) is N=100000. As seen in Figures 14(b), an AWGN with SNR=-5 dB is added to the pure signal. The system response is shown in Figure 14(c). Figure 15 is the same as Figure 14 but with an SNR of -15 dB. The detection probability of the   tochastic resonance method is based on energy of the calculated x(t).

Figure 16 shows the detection performance of SR method in terms of P_d. The performance of P_d versus SNR under different P_{fa} are given in Figure 16(a). The input SNR varies from -25 to 0 dB. As an

example, at SNR=-15 dB with P_{fa}=1% then P_d =96%. To further evaluating the detection performance, the ROC curves at SNR=-15 dB, -18 dB, and -21 dB are presented in Figure 16(b).
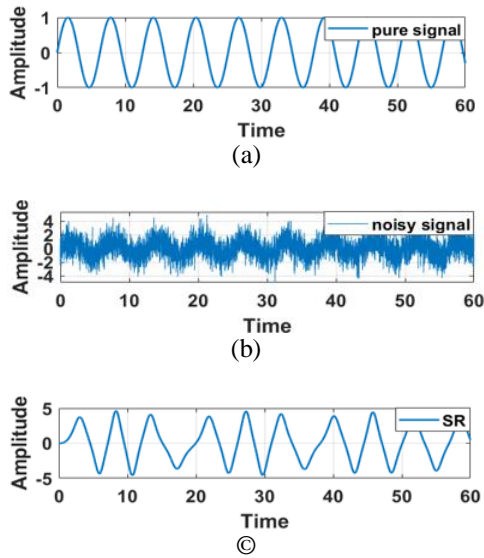

Figure 14. Detection of weak signals using SR method with SNR=-5 dB of: (a) pure signal wave, (b) noisy signal wave, and (c) SR output wave
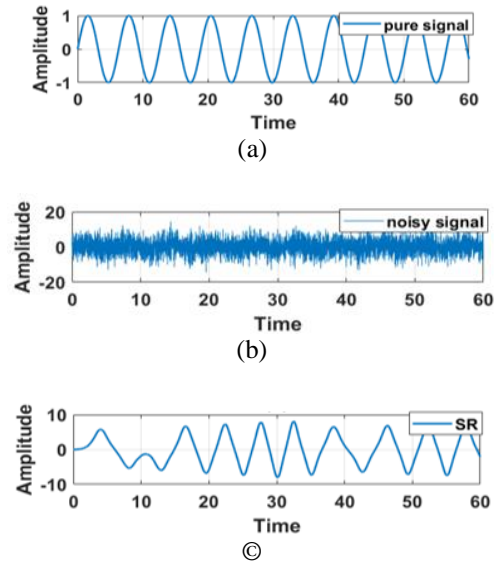
Figure 15. Detection weak signals using SR method with SNR=-15 dB of: (a) pure signal wave, (b) noisy signal wave, and (c) SR output wave
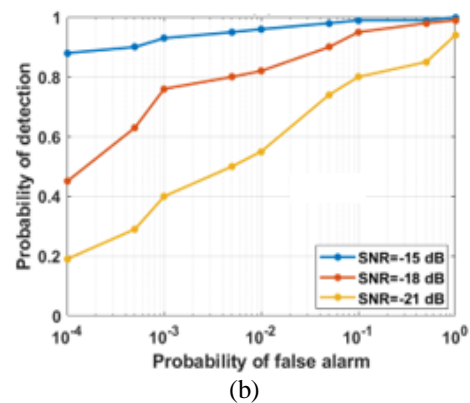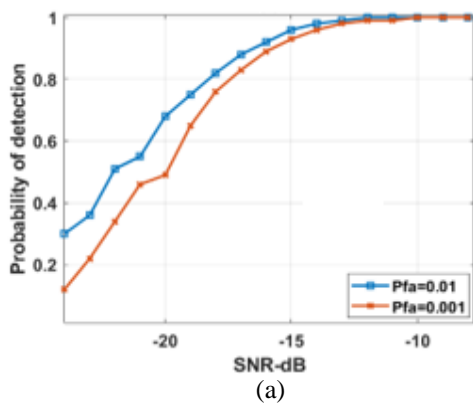

Figure 16. Performance of SR of (a) probability of detection versus SNR using SR method and (b) ROC performance curves of detection using SR method under SNR=-15 dB, -18 dB, and -21 dB

3.4. Comparison between previous techniques

Table 1 demonstrates a comparison of the SNR requirement for P_d=0.9 for P_{fa}=0.001, 0.005, and 0.01 for each signal detection techniques. One can easily notice that for P_d = 0.9, the Duffing osillator method is much better than wavelet mathod and stocastic resonance. Table 2 demonstrates a comparison of the coherency requirement and the order of the SNR required for detection.

Table 1. A comparison of SNR requirement at P_d=0.9 to keep P_{fa} at a specific value

Parameters	Duffing oscillator	Wavelet transform L=4	Stocastic resonance
SNR required for P_{fa} = 0.001	-78.2 dB	-15.1 dB	-15.5 dB
SNR required for P_{fa} = 0.005	-82.7 dB	-17.4 dB	-15.9 dB
SNR required for P_{fa} = 0.01	-89.6 dB	-18.2 dB	-16.2 dB

Table 2. A comparison of coherency and SNR requirements

Parameters	Duffing oscillator	Wavelet transform L=4	Stocastic resonance
Coherency	Yes	No	Yes
SNR range in dB ($P_d > 0.9$)	0 down to -80	0 down to -18	0 down to -16

4. CONCLUSION

In this paper, some of the techniques for detecting submerged weak signals in a stronge background noise are discussed. From the aforementioned, chaos theory works with very large noise levels, but this ability is canceled when the frequency is changed. As for wavelet transform, it is an easy-to-implement method for unknown signals, but its efficiency is limited by the problem of determining the basis wavelet. Finally, in this paper, stochastic resonance method is considered that gives good results compared to wavevlet transform, but it only works at a certain resonance frequency.

REFERENCES

[1] S. Li, Q. Shang, C. Yin, and Y. Qi, "Implementation of weak signal detection by Duffing oscillator in virtual instruments," in *Fifth International Symposium on Instrumentation and Control Technology*, Sep. 2003, vol. 5253, p. 536, doi: 10.1117/12.521840.

[2] Y. Li, B. J. Yang, J. Badal, X. P. Zhao, H. B. Lin, and R. L. Li, "Chaotic system detection of weak seismic signals," *Geophysical Journal International*, vol. 178, no. 3, pp. 1493–1522, Sep. 2009, doi: 10.1111/j.1365-246X.2009.04232.x.

[3] S. H. Shi, Y. Yuan, H. Q. Wang, and M. K. Luo, "Weak signal frequency detection method based on generalized Duffing oscillator," *Chinese Physics Letters*, vol. 28, no. 4, p. 040502, Apr. 2011, doi: 10.1088/0256-307X/28/4/040502.

[4] H. Shi, S. Fan, W. Xing, and J. Sun, "Study of weak vibrating signal detection based on chaotic oscillator in MEMS resonant beam sensor," *Mechanical Systems and Signal Processing*, vol. 50–51, pp. 535–547, Jan. 2015, doi: 10.1016/j.ymssp.2014.05.015.

[5] A. Wu, S. M. Mwachaka, Y. Pei, and Q. Fu, "A novel weak signal detection method of electromagnetic LWD based on a duffing oscillator," *Journal of Sensors*, vol. 2018, pp. 1–14, Jun. 2018, doi: 10.1155/2018/5847081.

[6] W. Luo, Q. Ou, F. Yu, L. Cui, and J. Jin, "Analysis of a new hidden attractor coupled chaotic system and application of its weak signal detection," *Mathematical Problems in Engineering*, vol. 2020, pp. 1–15, Dec. 2020, doi: 10.1155/2020/8849283.

[7] L. Shen, J. Xia, M. Ezawa, O. A. Tretiakov, G. Zhao, and Y. Zhou, "Signal detection based on the chaotic motion of an antiferromagnetic domain wall," *Applied Physics Letters*, vol. 118, no. 1, p. 012402, Jan. 2021, doi: 10.1063/5.0034997.

[8] S. G. Mallat, "A theory for multiresolution signal decomposition: the wavelet representation," *IEEE Transactions on Pattern Analysis and Machine Intelligence*, vol. 11, no. 7, pp. 674–693, Jul. 1989, doi: 10.1109/34.192463.

[9] N. Ehara, I. Sasase, and S. Mori, "Weak radar signal detection based on wavelet transform," *Electronics and Communications in Japan (Part III: Fundamental Electronic Science)*, vol. 77, no. 8, pp. 105–114, 1994, doi: 10.1002/ecjc.4430770810.

[10] J. Li, H. Li, and Z. Lei, "Research on the weak signal detection based on adaptive filtering of wavelet transform," *Procedia Engineering*, vol. 15, pp. 2583–2587, 2011, doi: 10.1016/j.proeng.2011.08.485.

[11] L. Ren, Y. L. Shi, R. L. Tian, and C. Y. Wang, "Study on radar weak signal detection method based on wavelet," *Applied Mechanics and Materials*, vol. 513–517, pp. 2967–2970, Feb. 2014, doi: 10.4028/www.scientific.net/AMM.513-517.2967.

[12] J. W. Shin, K. H. Song, K. S. Yoon, and H. N. Kim, "Weak radar signal detection based on variable band selection," *IEEE Transactions on Aerospace and Electronic Systems*, vol. 52, no. 4, pp. 1743–1755, Aug. 2016, doi: 10.1109/TAES.2016.150121.

[13] A. Z. Bin Abdullah *et al.*, "Wavelet based de-noising for on-site partial discharge measurement signal," *Indonesian Journal of Electrical Engineering and Computer Science*, vol. 16, no. 1, pp. 259–266, Oct. 2019, doi: 10.11591/ijeecs.v16.i1.pp259-266.

[14] N. H. Ja'afar and A. Ahmad, "Pipeline architectures of three-dimensional daubechies wavelet transform using hybrid method," *Indonesian Journal of Electrical Engineering and Computer Science*, vol. 15, no. 1, pp. 240–246, Jul. 2019, doi: 10.11591/ijeecs.v15.i1.pp240-246.

[15] A. M. Hamad Alhussainy and A. D. Jasim, "A novel pooling layer based on Gaussian function with wavelet transform," *Indonesian Journal of Electrical Engineering and Computer Science*, vol. 20, no. 3, pp. 1289–1298, Dec. 2020, doi: 10.11591/ijeecs.v20.i3.pp1289-1298.

[16] N. Zhang, P. Lin, and L. Xu, "Application of weak signal denoising based on improved wavelet threshold," *IOP Conference Series: Materials Science and Engineering*, vol. 751, no. 1, Jan. 2020, p. 012073, doi: 10.1088/1757-899X/751/1/012073.

[17] R. Benzi, A. Sutera, and A. Vulpiani, "The mechanism of stochastic resonance," *Journal of Physics A: Mathematical and General*, vol. 14, no. 11, pp. L453–L457, Nov. 1981, doi: 10.1088/0305-4470/14/11/006.

[18] B. McNamara and K. Wiesenfeld, "Theory of stochastic resonance," *Physical Review A*, vol. 39, no. 9, pp. 4854–4869, May 1989, doi: 10.1103/PhysRevA.39.4854.

[19] P. C. Etter, "Advanced applications for underwater acoustic modeling," *Advances in Acoustics and Vibration*, vol. 2012, pp. 1–28, May 2012, doi: 10.1155/2012/214839.

[20] Z. H. Lai and Y. G. Leng, "Generalized parameter-adjusted stochastic resonance of Duffing oscillator and its application to weak-signal detection," *Sensors (Switzerland)*, vol. 15, no. 9, pp. 21327–21349, Aug. 2015, doi: 10.3390/s150921327.

[21] F. Chapeau-Blondeau, "Input-output gains for signal in noise in stochastic resonance," *Physics Letters, Section A: General, Atomic and Solid State Physics*, vol. 232, no. 1–2, pp. 41–48, Jul. 1997, doi: 10.1016/S0375-9601(97)00350-2.

[22] Z. Gingl, P. Makra, and R. Vajtai, "High signal-to-noise ratio gain by stochastic resonance in a double well," *Fluctuation and Noise Letters*, vol. 01, no. 03, pp. L181–L188, Sep. 2001, doi: 10.1142/s0219477501000408.

[23] H. Dong, H. Wang, X. Shen, and Z. Jiang, "Effects of second-order matched stochastic resonance for weak signal detection," *IEEE Access*, vol. 6, pp. 46505–46515, 2018, doi: 10.1109/ACCESS.2018.2866170.

[24] S. Y. Ji, F. Yuan, K. Y. Chen, and E. Cheng, "Application of stochastic resonance technology in underwater acoustic weak signal detection," in *OCEANS 2016 - Shanghai*, Apr. 2016, pp. 1–5, doi: 10.1109/OCEANSAP.2016.7485567.

[25] X. Jiang, M. Diao, and S. Qu, "Signal detection algorithm design based on stochastic resonance technology under low signal-to-noise ratio," *Journal of Shanghai Jiaotong University (Science)*, vol. 24, no. 3, pp. 328–334, Jun. 2019, doi: 10.1007/s12204-019-2071-9.

[26] M. M. A. Jamil, A. A. Sadiq, M. S. Ahmad, N. A. M. Noor, N. A. A. Rahman, and N. Othman, "Magnetic particle imaging signal acquisition using second harmonic detection of magnetic nanoparticles," *Indonesian Journal of Electrical Engineering and Computer Science*, vol. 15, no. 1, pp. 221–229, Jul. 2019, doi: 10.11591/ijeecs.v15.i1.pp221-229.

[27] S. Lu, Q. He, and F. Kong, "Effects of underdamped step-varying second-order stochastic resonance for weak signal detection," *Digital Signal Processing: A Review Journal*, vol. 36, no. C, pp. 93–103, Jan. 2015, doi: 10.1016/j.dsp.2014.09.014.

[28] S. Zhao, P. Shi, and D. Han, "A novel mechanical fault signal feature extraction method based on unsaturated piecewise tri-stable stochastic resonance," *Measurement: Journal of the International Measurement Confederation*, vol. 168, p. 108374, Jan. 2021, doi: 10.1016/j.measurement.2020.108374.

[29] Y. Qiu, F. Yuan, S. Ji, and E. Cheng, "Stochastic resonance with reinforcement learning for underwater acoustic communication signal," *Applied Acoustics*, vol. 173, p. 107688, Feb. 2021, doi: 10.1016/j.apacoust.2020.107688.

BIOGRAPHIES OF AUTHORS

Sarah Sabah Mohammed was born in Baghdad, Iraq in 1994. She received the B.Sc. degree in electrical engineering in 2017 from the Mustansiriyah University, Iraq. Here research is to detect weak signal and signal processing in very low SNR. She can be contacted at email: eema1036@uomustansiriyah.edu.iq.

Prof. Maher K. Mahmoud Al-Azawi is the head of communications group/Elec. Engineering Department/College of Engineering/Al-mustansirayah University. He the author of more than 50 publications published in international and local journal and conferences. Most of them are within the subjects of digital communications, secure communications and digital speech and image processing. He can be contacted at email: maher.alazawi@uomustansiriyah.edu.iq.